Conf-9208144--3

DOE/MC/28055-93/C0135

# Recent Progress in Zirconia-Based Fuel Cells for Power Generation

Authors:
Singhal, S.C.

DOE/MC/28055--93/C0135

DE93 003488

Contractor:
Westinghouse Electric Corporation
Science & Technology Center
1310 Beulah Road
Pittsburgh, PA 15235-5098

Contract Number:
DE-FC21-91MC28055

Conference Title:
Fifth International Conference on the Science and Technology of Zirconia

Conference Location:
Melbourne, Australia

Conference Dates:
August 16-21, 1992

Conference Sponsor:
The Australian Ceramic Society

# DISCLAIMER

This report was prepared as an account of work sponsored by an agency of the United States Government. Neither the United States Government nor any agency thereof, nor any of their employees makes any warranty, express or implied, or assumes any legal liability or responsibility for the accuracy, completeness or usefulness of any information, apparatus, product, or process disclosed, or represents that its use would not infringe privately owned rights. Reference herein to any specific commercial product, process, or service by trade name, trademark, manufacturer, or otherwise, does not necessarily constitute or imply its endorsement, recommendation, or favoring by the United States Government or any agency thereof. The views and opinions of authors expressed herein do not necessarily state or reflect those of the United States Government or any agency thereof.

This report has been reproduced directly from the best available copy.

Available to DOE and DOE contractors from the Office of Scientific and Technical Information, P.O. Box 62, Oak Ridge, TN 37831; prices available from (615)576-8401, FTS 626-8401.

Available to the public from the National Technical Information Service, U.S. Department of Commerce, 5285 Port Royal Rd., Springfield, VA 22161.

# RECENT PROGRESS IN
# ZIRCONIA-BASED FUEL CELLS FOR POWER GENERATION

S. C. Singhal

Science and Technology Center
Westinghouse Electric Corporation
1310 Beulah Road
Pittsburgh, PA 15235, U.S.A.

## ABSTRACT

High temperature solid oxide fuel cells based upon yttria-stabilized zirconia electrolyte offer a clean, pollution-free technology to electrochemically generate electricity at high efficiencies. This paper reviews the designs, materials and fabrication processes used for such fuel cells. Most progress to date has been achieved with tubular geometry cells. A large number of tubular cells have been electrically tested, some to times up to 30,000 hours; these cells have shown excellent performance and performance stability. In addition, successively larger size electric generators utilizing these cells have been designed, built and operated since 1984. Two 25 kW power generation field test units have recently been fabricated; these units represent a major milestone in the commercialization of zirconia-based fuel cells for power generation.

## INTRODUCTION

The high oxygen ion conductivity over wide ranges of temperature and oxygen pressures in stabilized zirconia has led to its use as a solid oxide electrolyte in a variety of electrochemical applications. Zirconia-based oxygen sensors are widely used in combustion control, especially in automobiles, atmosphere control in furnaces, and as monitors of oxygen concentration in molten metals. Other applications include electrochemical pumps for control of oxygen potential, steam electrolyzers and high temperature solid oxide fuel cells (SOFC's).

High temperature fuel cells utilizing yttria-stabilized zirconia electrolyte offer a clean, pollution-free technology to electrochemically generate electricity at high efficiencies. These fuel cells provide many advantages over traditional energy conversion systems; these include high efficiency, reliability, modularity, fuel adaptability, and very low levels of $NO_x$ and $SO_x$ emissions. Furthermore, because of their high temperature of operation (~ $1000^{o}C$), these cells can be operated directly on natural gas eliminating the need for an expensive, external reformer system. These fuel cells also produce high quality exhaust heat which can be used for process heat or a bottoming electric power cycle to further increase the overall efficiency. This paper reviews the current status of the solid oxide fuel cell technology for power generation.

## OPERATING PRINCIPLE OF A SOLID OXIDE FUEL CELL

A solid oxide fuel cell essentially consists of two porous electrodes separated by a dense, oxygen ion conducting electrolyte. The operating principle of such a cell is illustrated in Figure 1. Oxygen supplied at the cathode (air electrode) reacts with incoming electrons from the external circuit to form oxygen ions, which migrate to the anode (fuel electrode) through the oxygen ion conducting electrolyte. At the anode, oxygen ions combine with $H_2$ (and/or CO) in the fuel to form $H_2O$ (and/or $CO_2$), liberating electrons. Electrons flow from the anode through the external circuit to the cathode. The reactions at the two electrodes can be written as follows:

Cathode: $1/2\,O_2 + 2\,e^- = O^{2-}$

Anode: $H_2 + O^{2-} = H_2O$

$CO + O^{2-} = CO_2$

The overall cell reaction is simply the oxidation of fuel ($H_2$ and/or CO) and the open circuit voltage, E, of the fuel cell is given by the Nernst equation:

$$E = \frac{RT}{4F} \ln \left\{ \frac{P_{O_2}\text{(oxidant)}}{P_{O_2}\text{(fuel)}} \right\}$$

where R is the gas constant, T is the cell temperature, F is the Faraday constant, and $Po_2$'s are the oxygen partial pressures. When a current passes through the cell, the cell voltage (V) is given by:

$$V = E - IR - \eta_A - \eta_F$$

where I is the current passing through the cell, R is the electrical resistance of the cell, and $\eta_A$ and $\eta_F$ are the polarization voltage losses associated with irreversibilities in electrode processes on the air side and the fuel side, respectively. To keep the IR loss low, the electrolyte in various solid oxide fuel cell designs is fabricated in the form of a thin film.

## DESIGNS OF SOLID OXIDE FUEL CELLS

Solid oxide fuel cells of several different designs are presently under development; these include planar, monolithic and tubular geometries.$^{(1-3)}$ The materials being considered for cell components in these different designs are either the same or very similar in nature.

In the planar design, illustrated in Figure 2, the cell components are configured as thin, flat plates. The interconnection having ribs on both sides forms gas flow channels and serves as bipolar gas separator contacting the anode and the cathode of adjoining cells. The dense electrolyte and interconnection are fabricated by tape casting, powder sintering or CVD,(4,5) whereas the porous electrodes are applied by slurry methods, screen printing, or by plasma spraying.(6) The planar cell design offers improved power density but requires high temperature gas seals at the edges of the plates to isolate oxidant from fuel. Difficulties in successfully developing such high temperature seals have limited the development and use of planar design cells for SOFC generators.

In the monolithic design also, the different cell components are fabricated as thin layers.(7) In the co-flow version of the monolithic solid oxide fuel cell, illustrated in Figure 3, the cell consists of a honeycomb-like array of adjacent fuel and oxidant channels. Such a cell is made of two types of laminated structures, anode/electrolyte/cathode and anode/interconnect/cathode. The anode/electrolyte/cathode composite is corrugated and stacked alternately between flat anode/interconnect/cathode composites. A cross-flow version of the monolithic solid oxide fuel cell, in which the fuel and oxidant flows are at right angle to each other, has also been investigated. Even though the monolithic solid oxide fuel cells offer potentially the highest power density of all SOFC designs, their fabrication involving co-sintering of the cell components at elevated temperatures has proven to be a formidable task. As a result, the development of large scale stacks utilizing monolithic solid oxide fuel cells has not progressed very far.

The most progress to date has been achieved with the tubular geometry fuel cell. Figure 4 illustrates the design of the Westinghouse tubular geometry cell. In this design, the active cell components are deposited in the form of thin layers on a ceramic support tube. The remaining sections in this paper relate to this tubular design solid oxide fuel cells.

## MATERIALS AND FABRICATION PROCESSES

The materials for different cell components have been selected based on the following criteria:

(a) Suitable electrical properties required of different cell components to perform their intended cell functions.

(b) Chemical stability at high temperatures during cell operation as well as during cell fabrication.

(c) Minimum reactivity and interdiffusion among different cell components.

(d) Matching thermal expansion among different cell components.

In addition to above materials selection criteria, the fabrication processes have been chosen so that every sequential component fabrication process does not affect those components already fabricated onto the support tube. The materials and fabrication processes used for different cell components are discussed below.

### Support Tube

The support tube acts both as a structural member onto which the active cell components are fabricated and as a functional member to allow the passage of air (or oxygen) to the air electrode (cathode) during cell operation. To perform both these functions, the support tube must have adequate mechanical integrity with sufficient porosity for gas permeation, must have matching thermal expansion with the air electrode, and should not react to any significant extent with the air electrode. To satisfy these requirements, a porous support tube (PST) made of zirconia stabilized with 15 mole percent calcia is used. The tube is made by extrusion of calcia-stabilized zirconia powder followed by sintering in air. The mechanical properties, e.g., rupture strength and elastic modulus, of these support tubes vary as a function of porosity.(8) To obtain sufficient strength such that the tubes can undergo all processing and operational conditions without structural failure and to provide adequate gas permeability, the tubes have about 35 percent porosity.

## Air Electrode (Cathode)

With operating temperature of around 1000°C in air or oxygen atmosphere, the material for the air electrode in solid oxide fuel cells has to meet the following requirements:

(a) High electronic conductivity.

(b) Chemical and dimensional stability in environments encountered during cell operation and during fabrication of interconnection, electrolyte and fuel electrode layers.

(c) Thermal expansion match with other cell components.

(d) Sufficient porosity and good adherence at the surface of the electrolyte.

(e) Compatibility and minimum reactivity with the support tube, the electrolyte and the interconnection with which air electrode comes into contact.

To satisfy these requirements, strontium-doped lanthanum manganite ($La_{0.9}Sr_{0.1}MnO_3$) is used as the air electrode material. Lanthanum manganite is a p-type perovskite oxide and shows reversible oxidation-reduction behavior. The material can have oxygen excess or deficiency depending upon the ambient oxygen partial pressure and temperature. Although, it is stable in air and oxidizing atmospheres, it dissociates at 1000°C at oxygen pressures $\leq 10^{-14}$ atm. The electronic conductivity of lanthanum manganite is due to small polaron hopping which is enhanced by doping with a divalent ion such as strontium. The defect chemistry, electrical conduction, and cathodic polarization behavior of doped lanthanum manganites have been studied in detail,(9,10) and strontium-doped lanthanum manganite has been found to satisfy all the requirements to be an effective air electrode. Furthermore, the reactivity and interdiffusion studies(11,12) between strontium-doped lanthanum manganite and yttria-stabilized zirconia electrolyte have shown any interactions between these two materials at 1000°C to be minimal.

The strontium-doped lanthanum manganite air electrode is deposited onto the calcia-stabilized zirconia support tube in the form of approximately 1.4 mm thick layer by a slurry filtration technique followed by sintering. To provide for adequate gas permeability, sintering conditions are controlled to achieve about 35 percent porosity in the air electrode.

## Electrolyte

Solid oxide fuel cells are based on the concept of an oxygen ion conducting electrolyte through which the oxygen ions migrate from the air electrode (cathode) side to the fuel electrode (anode) side where they oxidize the fuel ($H_2$, CO, etc.) to generate an electrical voltage. Zirconia doped with about 10 mole percent yttria is used as the electrolyte. Electrical properties and defect structure of yttria-stabilized zirconia have been thoroughly reviewed.(13,14) This material exhibits cubic fluorite structure in which yttrium ($Y^{3+}$) substitutes for the zirconium ($Zr^{4+}$) cations generating oxygen vacancies. The high ionic conductivity of yttria-stabilized zirconia is attributed to these oxygen ion vacancies along with low activation energy for oxygen ion migration. The conductivity of yttria-stabilized zirconia at 1000°C is maximum (about 0.1 $S \cdot cm^{-1}$) at about 10 mole percent yttria as shown by Strickler and Carlson;(15) the activation energy is also least near this composition. The thermal expansion of 10 mole percent yttria-stabilized zirconia is about $10 \times 10^{-6}/{}^{o}C$; materials for all other cell components are chosen to have thermal expansion near this value.

For optimum cell performance, the yttria-stabilized zirconia electrolyte must be free of porosity so as not to allow gases to permeate from one side of the electrolyte to the other, it should be uniformly thin to minimize ohmic loss, and it should have high oxygen ion conductivity with transport number for oxygen ions close to unity and a transport number for electrons as close to zero as possible. Electrolyte with these desired properties is deposited in the form of about 40 $\mu m$ thick layer by an electrochemical vapor deposition process. In this process, discussed in detail by Isenberg(16) and Pal and Singhal,(17) chlorides of zirconium and yttrium are volatilized in a predetermined ratio and passed along with hydrogen and argon over the outer surface of the porous air electrode. Oxygen mixed with steam at a predetermined ratio is passed inside the porous calcia-stabilized zirconia tube over which the porous air electrode is deposited. In the first stage of the reaction, designated as the chemical vapor deposition (CVD) stage, molecular diffusion of oxygen, steam, metal chlorides, and hydrogen occurs through the porous air electrode and these react to fill the pores in the air electrode with the yttria-stabilized zirconia electrolyte according to the following reactions:

$$2\ \mathrm{MeCl}_y + y\ \mathrm{H_2O} = 2\ \mathrm{MeO}_{y/2} + 2y\ \mathrm{HCl}$$

$$4\ \mathrm{MeCl}_y + y\ \mathrm{O_2} + 2y\ \mathrm{H_2} = 4\ \mathrm{MeO}_{y/2} + 4y\ \mathrm{HCl}$$

where Me is the cation species (zirconium and yttrium); and y is the valency associated with the cation. The temperature, the pressure and the different gas flow rates are so chosen that the above reactions are thermodynamically and kinetically favored.

During the second stage of the reaction after the pores in the air electrode are closed, electrochemical transport of oxygen ions maintaining electroneutrality occurs through the already deposited electrolyte in the pores from the high oxygen partial pressure side (oxygen/steam) to the low oxygen partial pressure side (chlorides). The oxygen ions, upon reaching the low oxygen partial pressure side, react with the metal chlorides and the electrolyte film grows in thickness. This second stage of the reaction is termed the electrochemical vapor deposition (EVD) stage.

The two stages of reaction, viz., the CVD stage and the EVD stage, responsible for the growth of the yttria-stabilized zirconia electrolyte film, are schematically shown in Figure 5. In this deposition process, the flows of the metal chloride vapors are maintained above a critical level to eliminate any gas-phase control of the EVD reaction. Furthermore, the ratio of yttrium chloride to zirconium chloride is so chosen that the electrolyte deposited contains about 10 mole percent yttria.

The growth of the electrolyte film is parabolic with time, as shown in Figure 6, and occurs by the oxygen ions diffusing through yttria-stabilized zirconia from the oxygen/steam side to the chlorides side. The rate controlling step in this process is the electronic transport (diffusion of electrons) through the electrolyte film; the average electronic transport number of the electrolyte during EVD at 1473 K is about $0.6 \times 10^{-4}$.(17) The electrochemical vapor deposition process ensures the formation of a pore-free, gas-tight, uniformly thick layer of the electrolyte over porous air electrode. A representative micrograph of the electrolyte layer over porous air electrode is shown in Figure 7.

## Fuel Electrode (Anode)

The fuel electrode of a solid oxide fuel cell must be electronically conducting, stable in the reducing environment of the fuel, and must have interconnected porosity to allow the passage of the fuel to the electrolyte surface. Due to the reducing atmosphere of the fuel gas, a metal such as nickel (or cobalt) can be used for SOFC anodes. However, the thermal expansion coefficient of nickel is considerably larger than that of the yttria-stabilized zirconia electrolyte; this large thermal expansion mismatch can cause delamination of the anode from the electrolyte surface. Also, nickel can sinter at the cell operating temperature resulting in a decrease in anode porosity. To circumvent these problems, a skeleton of yttria-stabilized zirconia is formed around the nickel particles. This skeleton of yttria-stabilized zirconia supports the nickel particles, inhibits sintering of the nickel particles during cell operation, provides adherence to the electrolyte, and also provides an anode thermal expansion coefficient closer to that of the electrolyte. Such nickel/yttria-stabilized zirconia anodes show very low diffusion and activation polarization losses during cell operation. Such anodes have also been shown to possess sufficient catalytic activity at 1000°C to reform natural gas and other hydrocarbons in situ.

A 100-150 $\mu$m thick layer of nickel/yttria-stabilized zirconia is applied over the electrolyte by a two-step process. In the first step, nickel powder is applied over the electrolyte by dipping in a nickel slurry. In the second step, yttria-stabilized zirconia is grown around the nickel particles by the same electrochemical vapor deposition process as used for depositing the electrolyte. A representative micrograph of the fuel electrode is shown in Figure 8. The fuel electrode contains 40 to 45 percent porosity.

## Interconnection

Interconnection, in the form of about 9 mm wide strip along the cell length, serves as the electric contact to the air electrode and also protects the air electrode material from the reducing environment of the fuel on the fuel electrode side. The requirements of the interconnection are most severe of all cell components and include:

(a) It should have nearly 100 percent electronic conductivity.

(b) Since it is exposed to air (or oxygen) on one side and fuel on the other, it should be stable in both oxidizing and reducing atmospheres at the cell operating temperature.

(c) It should have low permeability for oxygen and hydrogen to minimize direct combination of oxidant and fuel during cell operation.

(d) It should have a thermal expansion close to that of the air electrode and the electrolyte.

(e) It should be non-reactive with the air electrode, electrolyte and the electric contact material (e.g., nickel).

To satisfy these requirements, doped lanthanum chromite is used as the interconnection material. Lanthanum chromite is a p-type conductor; its conductivity is due to small polaron hopping from room temperature to 1400°C at oxygen pressures as low as $10^{-18}$ atm. The conductivity is enhanced as lower valence ions (e.g., Ca, Mg, Sr, etc.) are substituted on either the $La^{3+}$ or $Cr^{3+}$ sites. The defect chemistry, oxidation-reduction behavior, and the thermal expansion behavior of these chromites have been extensively studied.(9,18)

In the tubular solid oxide fuel cell, Mg-doped lanthanum chromite interconnection is deposited in the form of about 40 $\mu$m thick, 9 mm wide strip on the porous air electrode along the cell length by an electrochemical vapor deposition process,(16,19) similar to that used for depositing the electrolyte. This process ensures the deposition of a gas-tight, dense interconnection; a representative micrograph of the electrochemically vapor deposited magnesium-doped lanthanum chromite interconnection over porous air electrode is shown in Figure 9. This material has good electronic conductivity, low permeability for oxygen and hydrogen, and is stable in both oxidizing and reducing environments.(20)

Figure 10 shows the thermal expansion characteristics of the different cell components.(8) The thermal expansion of $La_{0.9}Sr_{0.1}MnO_3$ air electrode is closely matched to that of the calcia-stabilized zirconia support tube and the yttria-stabilized zirconia electrolyte. However, the thermal expansion of the Mg-doped lanthanum chromite interconnection is about 10-12 percent lower than that of other cell components. Better thermal expansion matching can be obtained if strontium-doped lanthanum chromite is used as the interconnection material.

Development efforts to reduce the cost of the cells utilizing alternate fabrication techniques and to increase the power output per cell are currently in progress.(21) Longer cells and increased power output per unit cell length are desirable to improve SOFC power plant economics. Over the past few years, the active length of the tubular SOFC has been increased from 30 cm (in pre- 1986 cells) to 100 cm (currently in production) with the result being a corresponding increase in power output per cell. In parallel with increasing the length, the thickness of the calcia-stabilized zirconia porous support tube (PST) has been reduced. Early technology tubular solid oxide fuel cells had a 2 mm wall thickness PST (the thick-wall PST). Although sufficiently porous to allow air flow to the air electrode, there was an inherent impedance to air flow toward air electrode. Efforts were successful in first reducing the PST wall thickness to 1.2 mm (the thin-wall PST) and ultimately in eliminating the PST altogether. As the PST wall thickness was reduced and the PST eventually eliminated from the cell, the air electrode thickness was increased. The present technology tubular solid oxide fuel cells have an air electrode tube onto which the other cell components are deposited. The combined effect of increasing the cell length from 30 cm to 100 cm and eliminating the PST has resulted in a six-fold (from 20 to 120 W) increase in power output per cell.(21)

## OPERATION AND PERFORMANCE OF A SOLID OXIDE FUEL CELL

The ceramic porous support tube is closed at one end. For cell operation, oxidant (air or oxygen) is introduced through a ceramic injector tube positioned inside the cell. The oxidant is discharged near the closed end of the cell and flows through the annular space formed by the cell and the coaxial injector tube. Fuel flows on the outside of the cell from the closed end and is electrochemically oxidized while flowing to the open end of the cell generating electricity.

At the open end of the cell, the oxygen-depleted air exits the cell and is combusted with the partially depleted fuel. Typically, 50 to 90 percent of the fuel is utilized in the electrochemical cell reaction. Part of the depleted fuel is recirculated in the fuel stream and the rest combusted to preheat incoming air and/or fuel to the fuel cell. The exhaust gas from the fuel cell is at 600 to 900°C depending on the operating conditions and can be used in a cogeneration system for producing process steam or in a steam turbine bottoming unit for an all-electric system.

A large number of single solid oxide fuel cells of the tubular design have been electrochemically tested(22) at 875 to 1200°C, some to times up to 30,000 hours, either on humidified hydrogen, a mixture of hydrogen and carbon monoxide, or natural gas. These cells have shown excellent performance and performance stability during long-term operation. A voltage-current plot at different temperatures is shown in Figure 11, and the power output as a function of current density for a 50 cm active length cell (with thin-wall porous support tube) is shown in Figure 12.

## SOLID OXIDE FUEL CELL GENERATOR SYSTEMS

To construct an electric generator, individual cells are connected in both parallel and series, as shown schematically in Figure 13, to form a semi-rigid bundle that is the basic building block of a generator. Nickel felt, consisting of long nickel metal fibers sinter bonded to each other, is used to provide soft, mechanically compliant, low electrical resistance connections between the cells. This material bonds to the nickel particles in the fuel electrode and the nickel plating on the interconnection for the series connection, and to the two adjacent cell fuel electrodes for the parallel connection; such a series-parallel arrangement provides improved generator reliability. The individual cell bundles are arrayed in series to build voltage and form generator modules. These modules are further combined in either series or parallel to form large scale generators.

Figure 14 illustrates the basic design concept of the Westinghouse seal-less solid oxide fuel cell generator.(23,24) Fuel is introduced to a plenum at the bottom and flows upward between the cells. This fuel is electrochemically oxidized producing electricity and heat as it flows past the cells. Spent fuel and oxidation products (e.g., $CO_2$ and $H_2O$) enter the spent fuel combustion chamber located above the cells. Air is introduced to a plenum at the top of the generator. From the air plenum, air enters the air injector tubes which are suspended, one per cell, from the air plenum into the cells. After passing inside the cells, the air depleted in oxygen, exits from the open end of the cells into the same chamber as the spent fuel, combusting the spent fuel and producing additional heat which is used to preheat the incoming air. The exhaust products exit the generator from this chamber at temperatures up to 900°C depending upon operating conditions.

The seal-less generator concept has been tested in a number of different-size generators, as summarized in Table I. In 1984, a 400 W generator consisting of two 12-cell bundles connected in electrical series was tested(23,24) for about 2,000 hours. During operation, this generator was cycled five times to approximately room temperature and back to operating temperature (about 1000°C). The successful test of this generator was followed by the design, construction and test, in late 1986, of a larger 5 kW generator consisting of 324 cells.(24) This generator was tested for about 500 hours, and achieved 5.2 kW at 80 amperes with 6 stoichs air and 85% fuel (66.6% $H_2$, 22.2% CO and 11.1% $H_2O$) utilization at 1000°C.

Additional SOFC generators have been designed, built and delivered for field testing by prospective customers of large-scale SOFC power generation systems. The Tennessee Valley Authority (TVA) acquired the first such unit for the purposes of demonstrating the capabilities of the technology and providing independent corroboration of overall performance and reliability. This 400 W generator, consisting of 24 cells arranged in two series connected bundles, was tested(25,26) in early 1987 for about 1,760 hours over a range of currents, fuel utilizations, air flows and temperatures, and demonstrated the capability of the system to satisfy its design requirements for automatic unattended operation and load follow.

Subsequently, Tokyo Gas and Osaka Gas each acquired a 3 kW SOFC generation system in 1987. Each system consisted of an SOFC generator module containing 144 cells, electrical air pre-heaters for generator temperature control, air and fuel handling systems and a computer-based control system.(26) The generators could be run on hydrogen, a mixture of hydrogen and carbon monoxide, or the effluent from a customer supplied fuel gas supply such as a methane reformer. The testing and performance of these systems has been discussed in detail by Veyo,(26) Harada and Mori,(27) and Yamamoto, et al.(28) In brief, each of these systems produced 3 kW of dc power as designed; the system at Tokyo Gas operated continuously and successfully for over six months. The system at Osaka Gas operated continuously for 3,700 hours before being shut down for external (non-SOFC) causes.

In 1989, another 3 kW generator, again consisting of 144 cells, was fabricated to operate on desulfurized pipeline natural gas; this generator incorporated an integrated, internal reformer and partial recirculation of depleted fuel.(29) The generator was operated successfully for over 5,400 hours, and either met or exceeded the design goals.

In 1990, a 20 kW generator, the first SOFC generator of a commercially meaningful size, was fabricated. This generator consisted of 576 cells of 50 cm active length, and also incorporated an integrated, internal reformer and partial recirculation of depleted fuel. This generator was successfully operated for a total of 3,355 hours on three different fuels - hydrogen, desulfurized pipeline natural gas and naphtha – producing up to 20 kW.(30)

In early 1992, a 25 kW dc power generator, consisting of 1,152 cells of 50 cm active length, was fabricated and delivered for testing at Rokko Island, near Osaka, Japan, in a joint program with Kansai Electric Power Company (KEPCO), Osaka Gas Company (OG) and Tokyo Gas Company (TG). The cells in this generator are contained in two independently controlled and operated units. A second 25 kW SOFC system, a cogeneration unit supported by Osaka Gas Company and Tokyo Gas Company, has been fabricated; this system will supply ac power and intermediate pressure steam to another test site in Japan. These two 25 kW units represent a major milestone in the commercialization of zirconia-based fuel cells for power generation.

## SUMMARY

High temperature solid oxide fuel cells based on yttria-stabilized zirconia electrolyte offer many advantages over traditional energy systems. These include high conversion efficiency, reliability, modularity, fuel adaptability and virtually unlimited siteability due to very low $NO_x$ emissions.(31) Furthermore, these cells produce high quality exhaust heat which can be used for process heat or a bottoming electric power cycle to further increase the overall plant efficiency.

Westinghouse has developed the materials and fabrication processes for these fuel cells, and has successfully employed and tested these cells for power generation in successively larger generators. When fully commercialized, the zirconia-based fuel cell systems are expected to serve a wide range of power and heat applications, such as large-scale power generation by electric and gas utilities and industrial cogeneration.

## ACKNOWLEDGEMENTS

The author acknowledges the contributions of his many colleagues whose work is reviewed in this paper. The development of solid oxide fuel cell technology has been supported by the U.S. Department of Energy (DOE), the Gas Research Institute (GRI), the Westinghouse Electric Corporation, and various utility and industry sources.

## REFERENCES

1. S. C. Singhal, (ed.), Solid Oxide Fuel Cells, The Electrochemical Society, Inc., Pennington, NJ, (1989), pp. 279-383.

2. A. J. Appleby and F. R. Foulkes, Fuel Cell Handbook, Van Nostrand Reinhold, New York, NY, (1989), pp. 579-611.

3. F. Grosz, P. Zegers, S. C. Singhal and O. Yamamoto, (eds.), Proceedings of the Second International Symposium on Solid Oxide Fuel Cells, Commission of the European Communities, Luxembourg, (1991), pp. 1-112.

4. P. A. Lessing, L. W. Tai and K. A. Klemm, "Fabrication Technologies for a Planar Solid Oxide Fuel Cell", in Solid Oxide Fuel Cells, (S. C. Singhal, ed.), The Electrochemical Society, Inc., Pennington, NJ, (1989), pp. 337-360.

5. C. Milliken and A. Khandkar, "Fabrication of Integral Flow Field/Interconnects for Planar SOFC Stacks", in Solid Oxide Fuel Cells, (S. C. Singhal, ed.), The Electrochemical Society, Inc., Pennington, NJ, (1989), pp. 361-376.

6. H. Arai, "Solid Oxide Fuel Cells with Stabilized Zirconia Thick Films Fabricated by Various Techniques", in Proceedings of SOFC-Nagoya, Japan Fine Ceramics Center, Nagoya, Japan, (1989), pp. 9-14.

7. N. Q. Minh, C. R. Horne, F. Liu, P. R. Staszak, T. L. Stillwagon and J. J. Van Ackeren, "Forming and Processing of Monolithic Solid Oxide Fuel Cells", in Solid Oxide Fuel Cells, (S. C. Singhal, ed.), The Electrochemical Society, Inc., Pennington, NJ, (1989), pp. 307-316.

8. A. O. Isenberg, "Technology Status of High-Temperature Solid Oxide Fuel Cells and Electrolyzers", in Proceedings International Symposium on Fine Ceramics, Arita, Japan, (1988), pp. 107-122.

9. H. U. Anderson, J. H. Kuo and D. M. Sparlin, "Review of Defect Chemistry of $LaMnO_3$ and $LaCrO_3$", in Solid Oxide Fuel Cells, (S. C. Singhal, ed.), The Electrochemical Society, Inc., Pennington, NJ, (1989), pp. 111-128.

10. O. Yamamoto, Y. Takeda, R. Kanno and M. Noda, "Perovskite Type Oxides as Oxygen Electrodes for High Temperature Oxide Fuel Cells", Solid State Ionics, Vol. 22, (1987), pp. 241-246.

11. S. K. Lau and S. C. Singhal, "Potential Electrode/Electrolyte Interactions in Solid Oxide Fuel Cells", Corrosion 85, Paper No. 345, (1985), pp. 1-9.

12. O. Yamamoto, Y. Takeda, R. Kanno and T. Kojima, "Stability of Perovskite Oxide Electrode with Stabilized Zirconia", in Solid Oxide Fuel Cells, (S. C. Singhal, ed.), The Electrochemical Society, Inc., Pennington, NJ, (1989), pp. 242-253.

13. R. M. Dell and A. Hooper, "Oxygen Ion Conductors", in Solid Electrolytes, (P. Hagenmuller and W. van Gool, eds.), Academic Press, New York, NY, (1978), pp. 291-312.

14. E. C. Subbarao and H. S. Maiti, "Solid Electrolytes with Oxygen Ion Conduction", Solid State Ionics, Vol. 11, (1984), pp. 317-338.

15. D. W. Strickler and W. G. Carlson, "Ionic Conductivity of Cubic Solid Solutions in the System $CaO-Y_2O_3-ZrO_2$", J. American Ceramic Soc., Vol. 47 (3), (1964), pp. 122-127.

16. A. O. Isenberg, "Growth of Refractory Oxide Layers by Electrochemical Vapor Deposition (EVD) at Elevated Temperatures", in Electrode Materials and Processes for Energy Conversion and Storage, (J. D. E. McIntyre, S. Srinivasan and F. G. Will, eds.), The Electrochemical Society, Inc., Princeton, NJ, Vol. 77-6, (1977), pp. 572-583.

17. U. B. Pal and S. C. Singhal, "Electrochemical Vapor Deposition of Yttria-Stabilized Zirconia Films", J. Electrochem. Soc., Vol. 137, (1990), pp. 2937-2941.

18. S. Srilomsak, D. P. Schilling and H. U. Anderson, "Thermal Expansion Studies on Cathode and Interconnect Oxides", in Solid Oxide Fuel Cells, (S. C. Singhal, ed.), The Electrochemical Society, Inc., Pennington, NJ, (1989), pp. 129-140.

19. U. B. Pal and S. C. Singhal, "Growth of Perovskite Films by Electrochemical Vapor Deposition", High Temp. Science, Vol. 27, (1990), pp. 251-264.

20. S. C. Singhal, R. J. Ruka and S. Sinharoy, "Interconnection Materials Development for Solid Oxide Fuel Cells", U.S. Department of Energy Final Report DOE/MC/21184-1985, (1985), 54 pages.

21. E. Ray, "High Temperature Tubular Solid Oxide Fuel Cell Development", in Proceedings Fourth Annual Fuel Cell Contractors Review Meeting, (W. J. Huber, ed.), U.S. Department of Energy, Morgantown, WV, (1992), in press.

22. N. J. Maskalick, "Design and Performance of Tubular Solid Oxide Fuel Cells", in Solid Oxide Fuel Cells, (S. C. Singhal, ed.), The Electrochemical Society, Inc., Pennington, NJ, (1989), pp. 279-287.

23. G. E. Zymboly, P. Reichner and J. M. Makiel, "Cell Fabrication, Design, and Operation of a Solid Oxide Fuel Cell Generator", in National Fuel Cell Seminar Abstracts, Courtesy Associates, Inc., Washington, DC, (1985), pp. 95-101.

24. P. Reichner and J. M. Makiel, "Development Status of Multi-Cell Solid Oxide Fuel Cell Generators", in National Fuel Cell Seminar Abstracts, Courtesy Associates, Inc., Washington, DC, (1986), pp. 32-35.

25. D. R. Stephenson, Jr. and S. E. Veyo, "TVA Test of SOFC Subscale Generator", in National Fuel Cell Seminar Abstracts, Courtesy Associates, Inc., Washington, DC, (1986), pp. 36-39.

26. S. E. Veyo, "SOFC Field Experiments, A Learning Experience", in National Fuel Cell Seminar Abstracts, Courtesy Associates, Inc., Washington, DC, (1988), pp. 13-17.

27. M. Harada and Y. Mori, "Osaka Gas Test of 3 kW SOFC Generator System", in National Fuel Cell Seminar Abstracts, Courtesy Associates, Inc., Washington, DC, (1988), pp. 18-21.

28. Y. Yamamoto, S. Kaneko, and H. Takahashi, "Tokyo Gas Tests of 3 kW Generation Systems", in National Fuel Cell Seminar Abstracts, Courtesy Associates, Inc., Washington, DC, (1988), pp. 25-28.

29. L. A. Shockling and J. M. Makiel, "Natural Gas-Fueled 3 kWe SOFC Generator Test Results", in Proceedings of the 25th Intersociety Energy Conversion Engineering Conference, (P. A. Nelson, W. W. Schertz and R. H. Till, eds.), American Institute of Chemical Engineering, New York, NY, Vol. 3, (1990), pp. 224-229.

30. W. J. Dollard, "Solid Oxide Fuel Cell Development at Westinghouse", J. Power Sources, Vol. 37, (1992), pp. 133-139.

31. S. C. Singhal, "Solid Oxide Fuel Cells for Clean and Efficient Power Generation", in Proceedings of the Fukuoka International Symposium on Global Environment and Energy Issues, (T. Seiyama, ed.), The Electrochemical Society of Japan, Fukuoka, Japan, (1990), pp. 95-104.

Table I - Summary of Westinghouse SOFC Generator Systems

| Customer | Size (kW) | No. of Cells | Cell Length (cm) | Test Time (hrs) | Year |
|---|---|---|---|---|---|
| U.S. DOE | 0.4 | 24 | 30 | 2,000 | 1984 |
| U.S. DOE | 5.0 | 324 | 30 | 500 | 1986 |
| TVA | 0.4 | 24 | 30 | 1,760 | 1987 |
| Tokyo Gas (TG) | 3.0 | 144 | 36 | 5,000 | 1987-88 |
| Osaka Gas (OG) | 3.0 | 144 | 36 | 3,700 | 1987-88 |
| GRI | 3.0 | 144 | 36 | 5,400 | 1989-90 |
| U.S. DOE | 20.0 | 576 | 50 | 3,355 | 1990-91 |
| KEPCO/TG/OG | 25.0* | 1,152 | 50 | -- | 1992 |
| TG/OG | 25.0* | 1,152 | 50 | -- | 1992 |

* Nominal rating. Capable of producing 40 kW at peak operation.

# LIST OF FIGURE CAPTIONS

Figure 1 - Operating principle of a solid oxide fuel cell.

Figure 2 - Cross-flow planar solid oxide fuel cell design.

Figure 3 - Co-flow monolithic solid oxide fuel cell design.

Figure 4 - Tubular solid oxide fuel cell design.

Figure 5 - Two stages of reaction occurring during the deposition of the yttria-stabilized zirconia electrolyte.

Figure 6 - Growth kinetics of the yttria-stabilized zirconia electrolyte by the electrochemical vapor deposition process at 1473 K.

Figure 7 - Representative micrograph of the electrochemically vapor deposited yttria-stabilized zirconia electrolyte over porous air electrode.

Figure 8 - Representative micrograph of the nickel/yttria-stabilized zirconia fuel electrode over the electrolyte.

Figure 9 - Representative micrograph of the electrochemically vapor deposited Mg-doped lanthanum chromite interconnection over porous air electrode.

Figure 10 - Thermal expansion of materials in the tubular solid oxide fuel cell.

Figure 11 - Voltage-current curves at different temperatures for 50 cm active length thin-wall PST cells.

Figure 12 - Power output as a function of current density for a 50 cm active length thin-wall PST cell.

Figure 13 - Cell cross-sections showing series and parallel electrical connections.

Figure 14 - Solid oxide fuel cell seal-less generator concept.

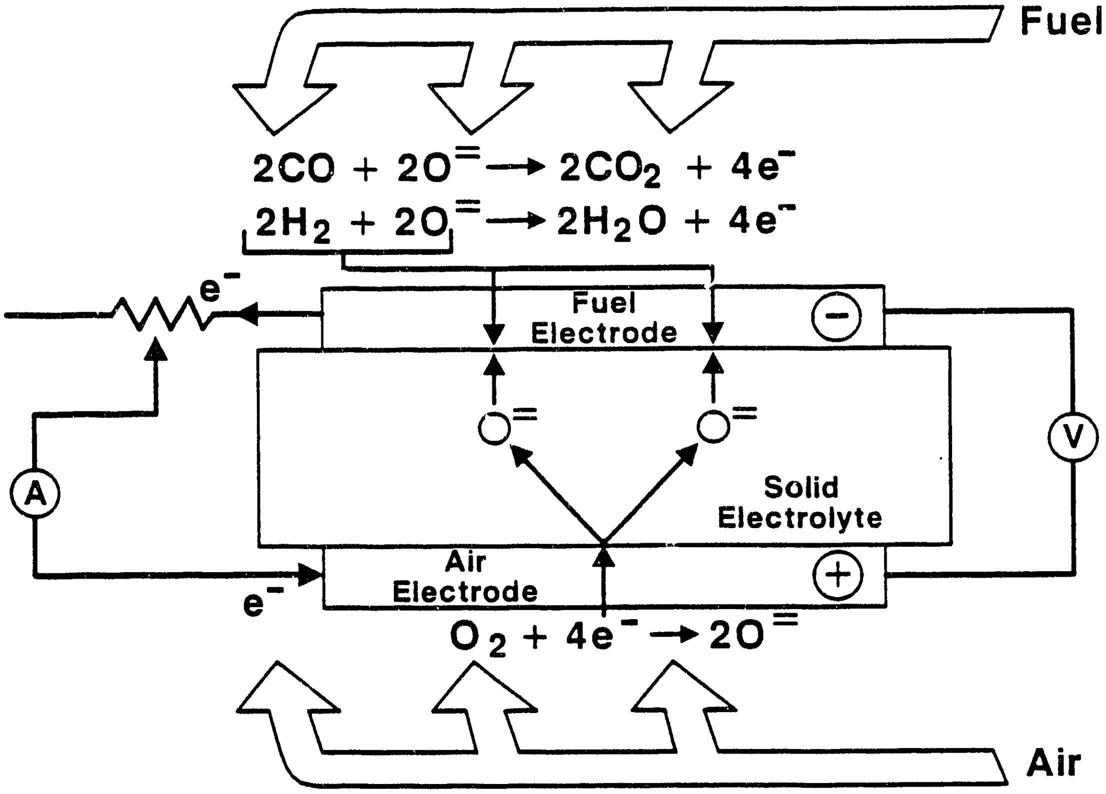

Figure 1 - Operating principle of a solid oxide fuel cell.

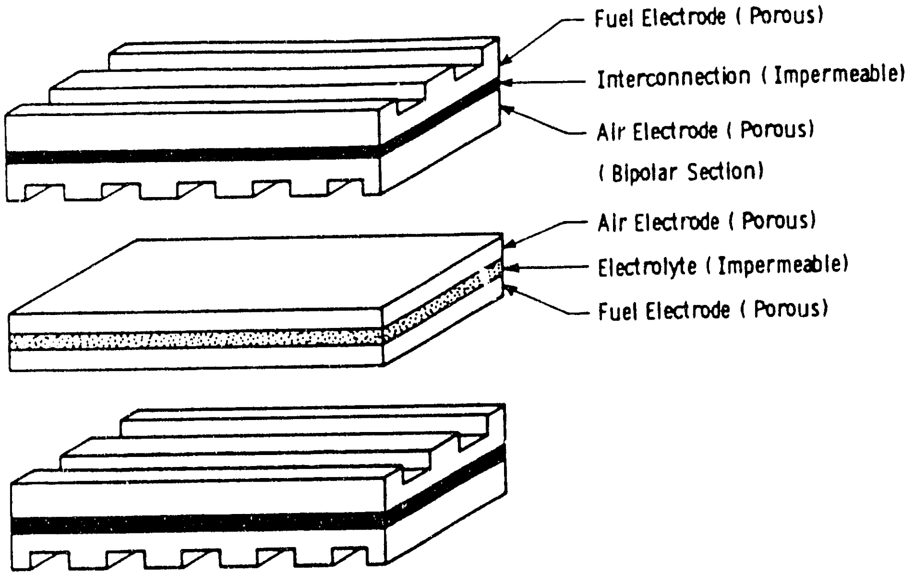

Figure 2 - Cross-flow planar solid oxide fuel cell design.

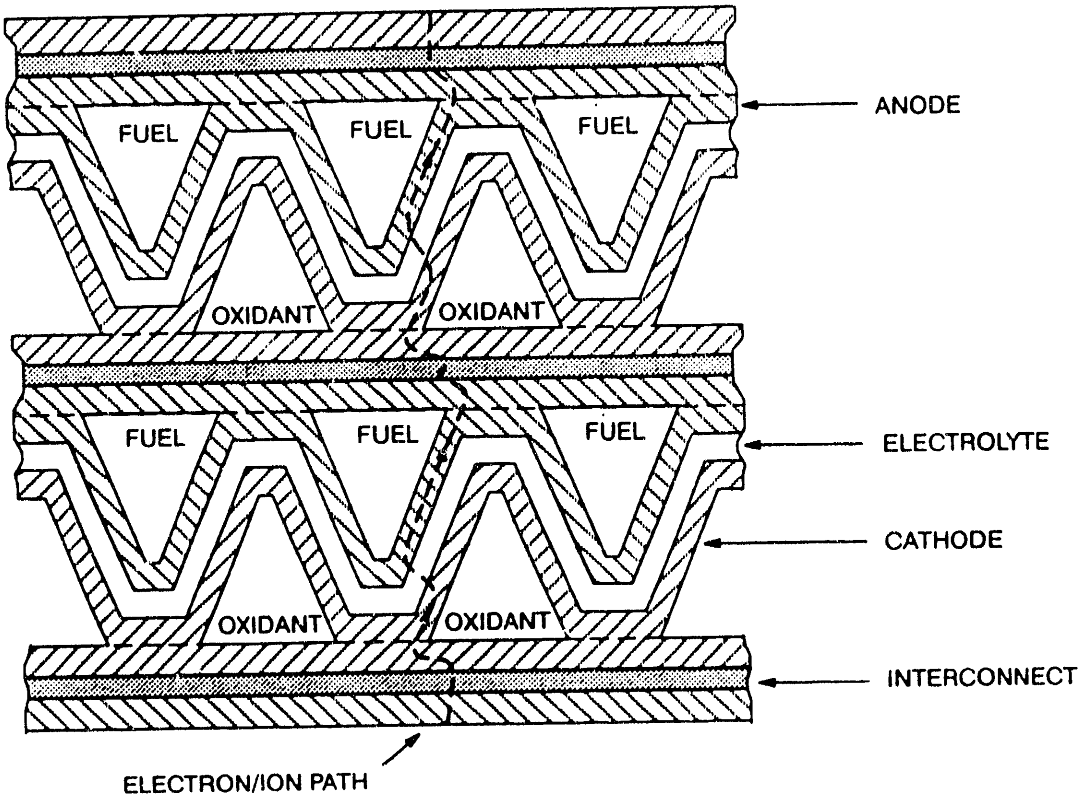

Figure 3 - Co-flow monolithic solid oxide fuel cell design.

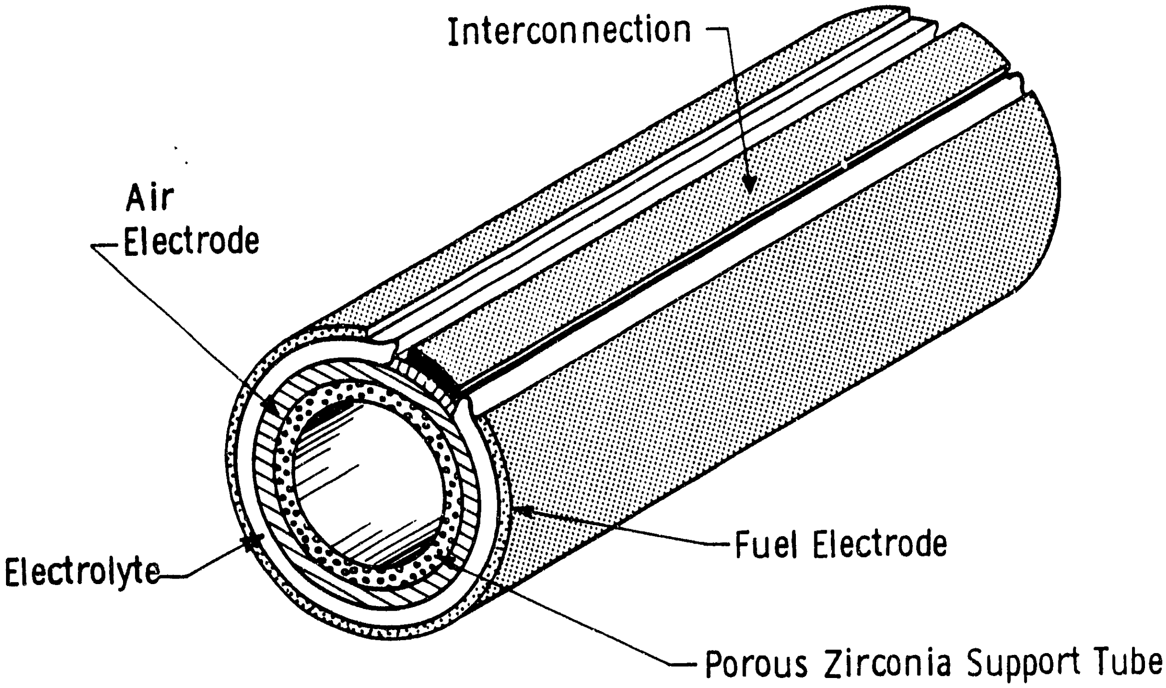

Figure 4 - Tubular solid oxide fuel cell design.

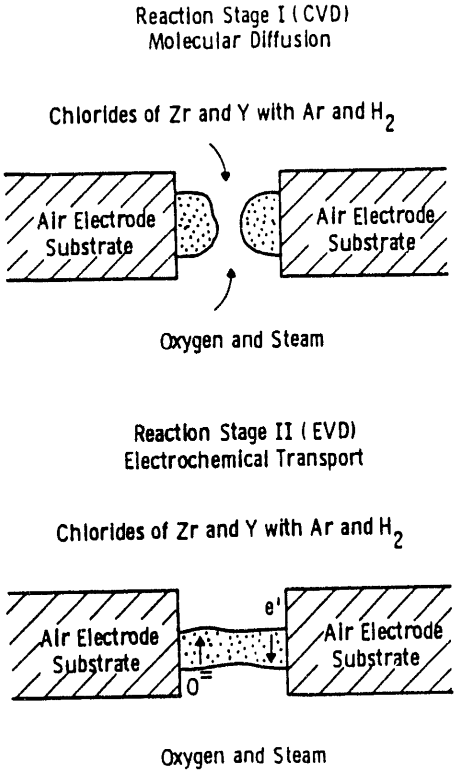

Figure 5 - Two stages of reaction occurring during the deposition of the yttria-stabilized zirconia electrolyte.

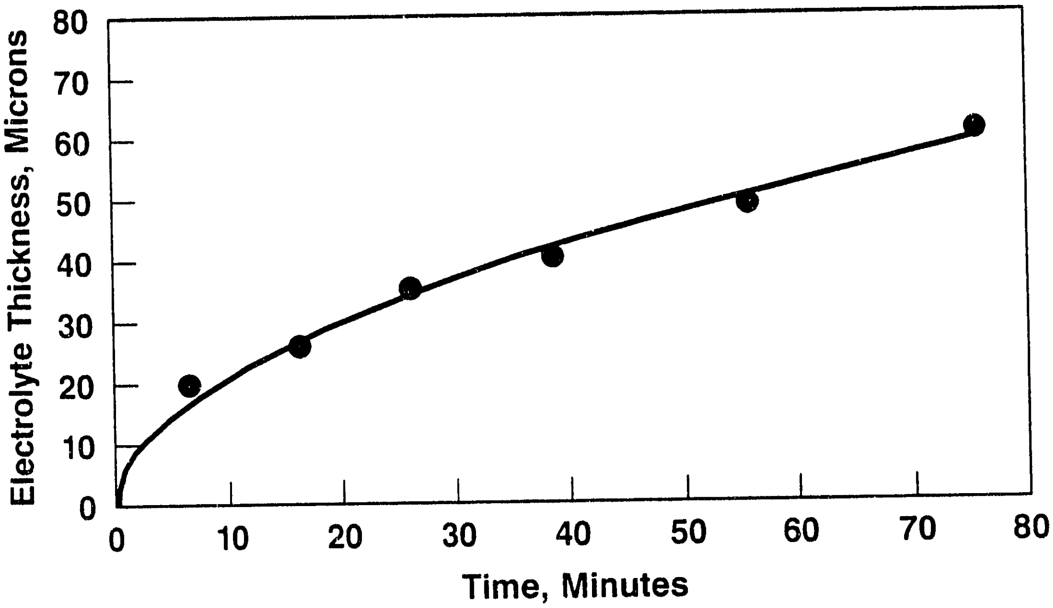

Figure 6 - Growth kinetics of the yttria-stabilized zirconia electrolyte by the electrochemical vapor deposition process at 1473 K.

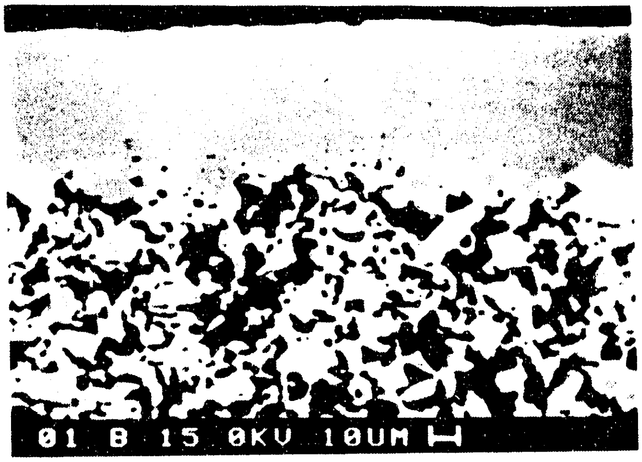

Figure 7 - Representative micrograph of the electrochemically vapor deposited yttria-stabilized zirconia electrolyte over porous air electrode.

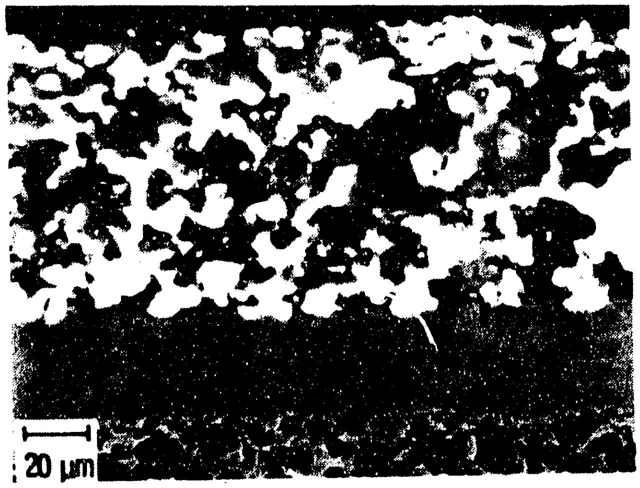

Figure 8 - Representative micrograph of the nickel/yttria-stabilized zirconia fuel electrode over the electrolyte.

Figure 9 - Representative micrograph of the electrochemically vapor deposited Mg-doped lanthanum chromite interconnection over porous air electrode.

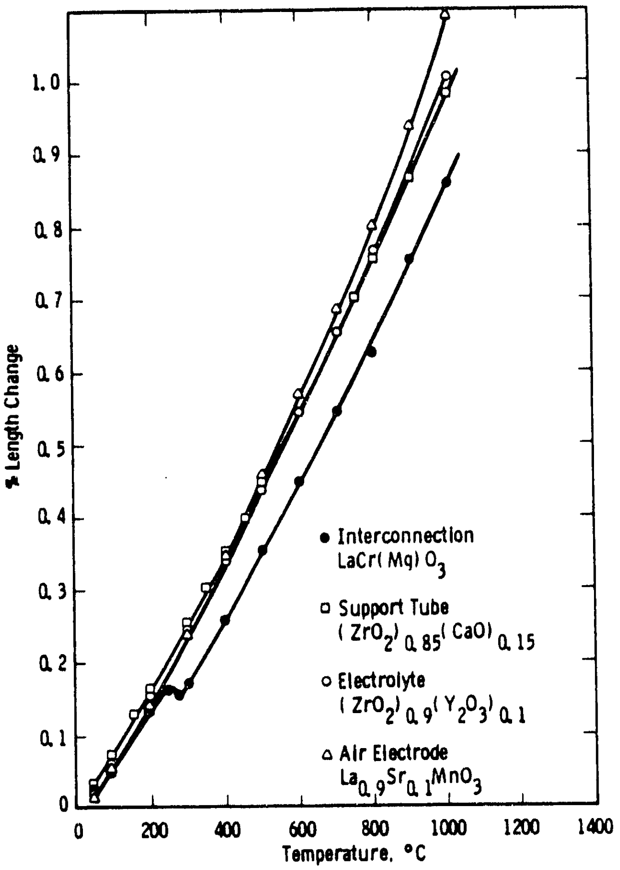

Figure 10 - Thermal expansion of materials in the tubular solid oxide fuel cell.

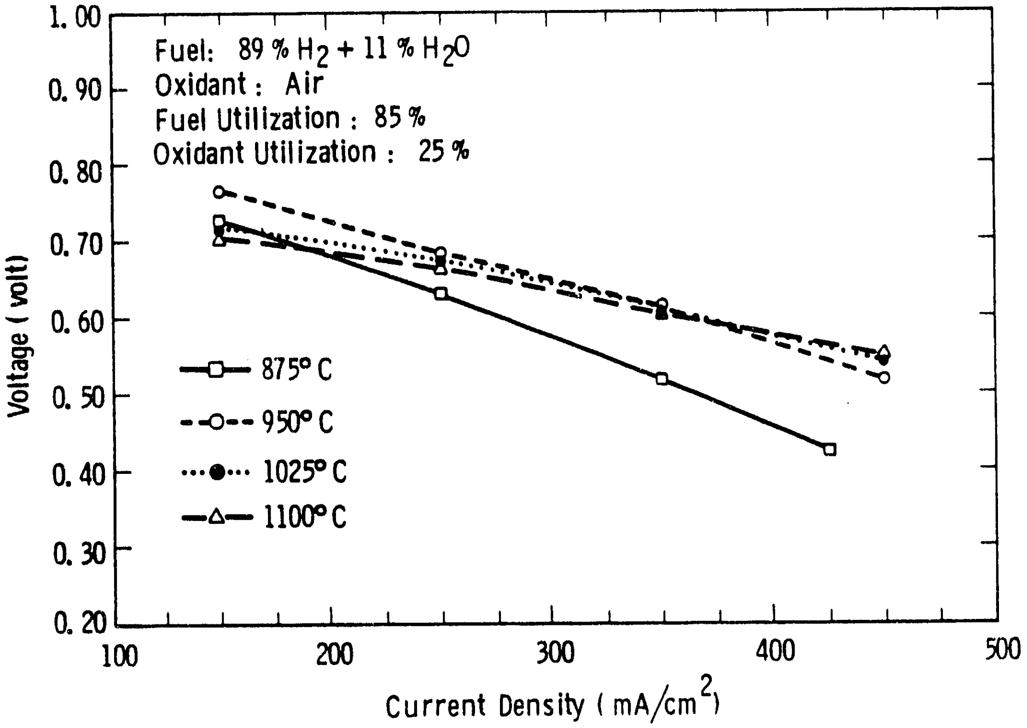

Figure 11 - Voltage-current curves at different temperatures for 50 cm active length thin-wall PST cells.

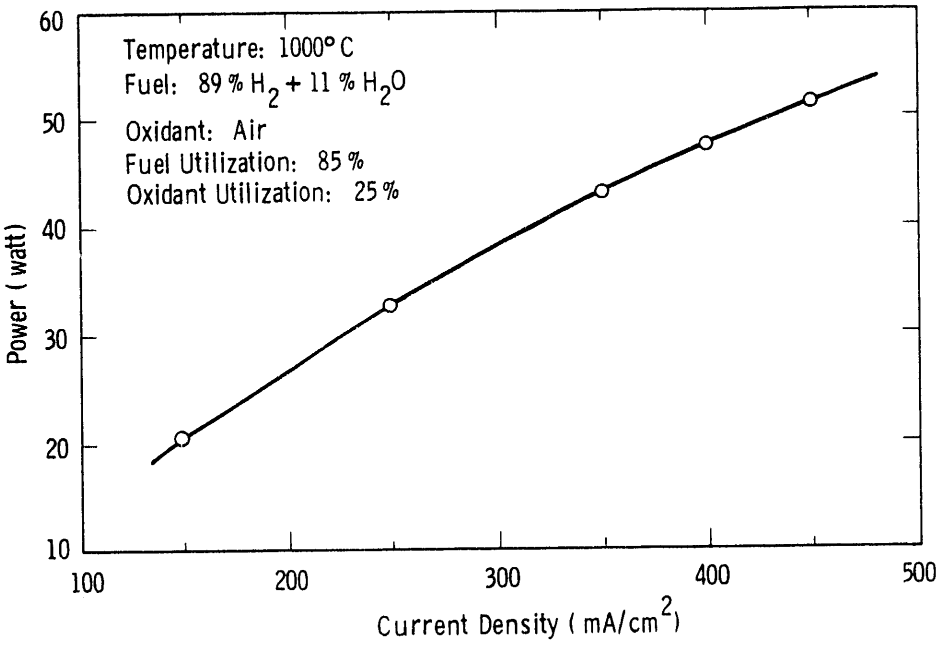

Figure 12 - Power output as a function of current density for a 50 cm active length thin-wall PST cell.

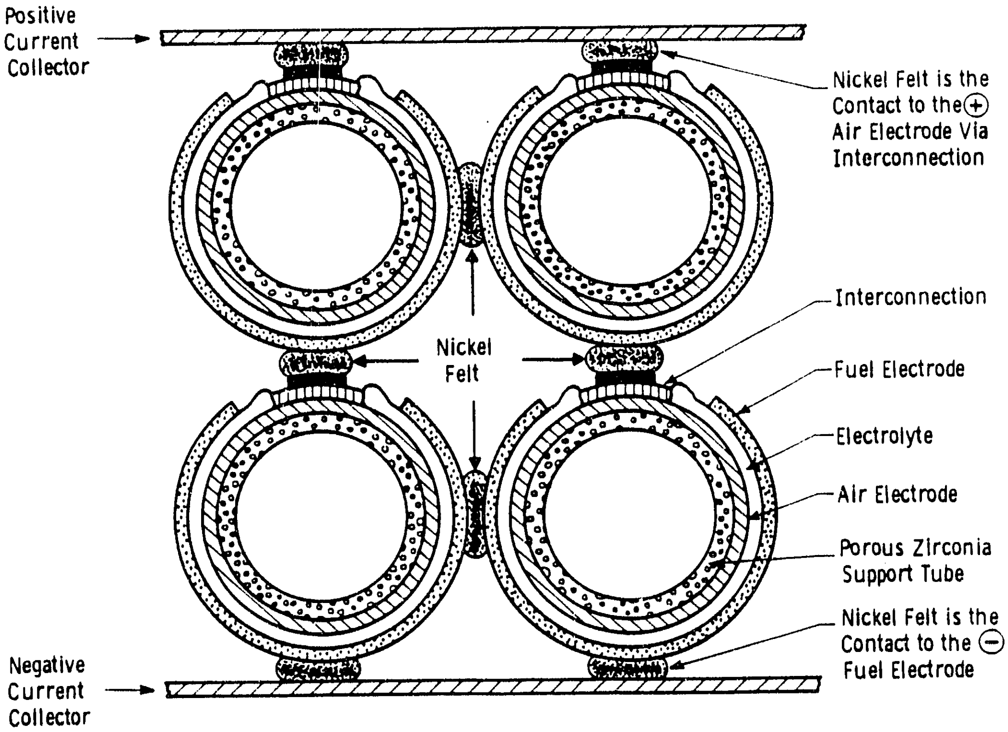

Figure 13 - Cell cross-sections showing series and parallel electrical connections.

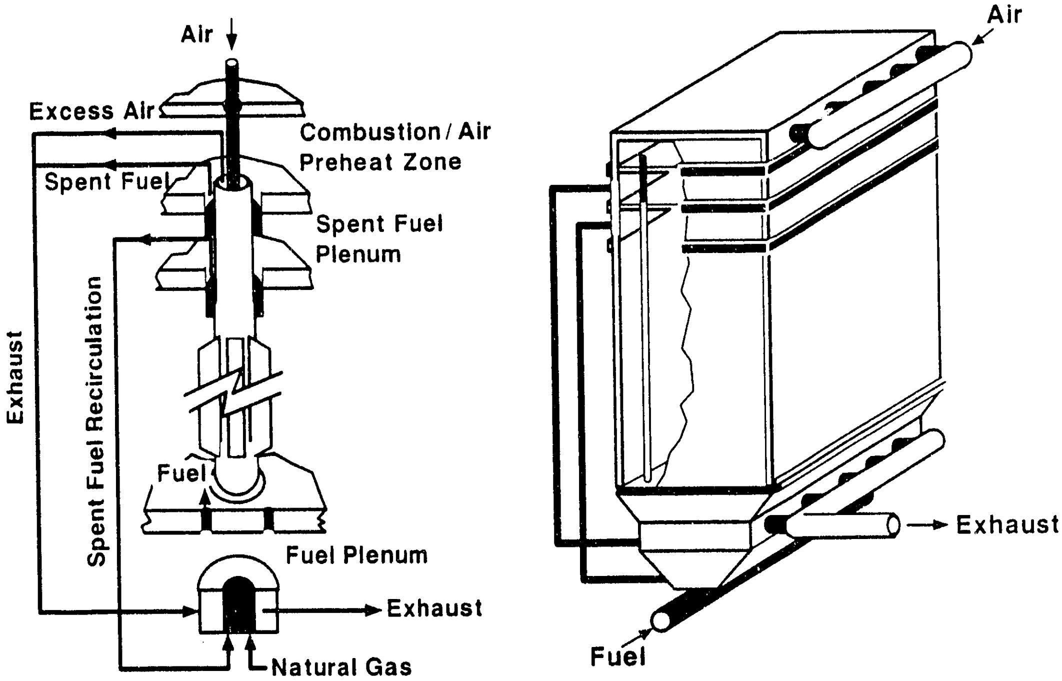

Figure 14 - Solid oxide fuel cell seal-less generator concept.

# END

DATE FILMED

2 / 10 / 93